

Photoelectron diffraction determination of the structure of the Cu(100) $c(2 \times 2)$ - Mn surface phase

This article has been downloaded from IOPscience. Please scroll down to see the full text article.

1996 J. Phys.: Condens. Matter 8 10231

(<http://iopscience.iop.org/0953-8984/8/49/014>)

View [the table of contents for this issue](#), or go to the [journal homepage](#) for more

Download details:

IP Address: 171.66.16.207

The article was downloaded on 14/05/2010 at 05:47

Please note that [terms and conditions apply](#).

Photoelectron diffraction determination of the structure of the Cu(100)c(2 × 2)–Mn surface phase

R Toomes[†], A Theobald[‡], R Lindsay[‡], T Geißel[‡], O Schaff[‡], R Didszhun[‡],
D P Woodruff[†], A M Bradshaw[‡] and V Fritzsche[§]

[†] Physics Department, University of Warwick, Coventry CV4 7AL, UK

[‡] Fritz-Haber-Institut der Max-Planck-Gesellschaft, Faradayweg 4-6, 14195 Berlin (Dahlem), Germany

[§] Institut für Theoretische Physik, Technische Universität Dresden, 01062 Dresden, Germany

Received 24 July 1996

Abstract. The structure of the Cu(100)c(2 × 2)–Mn surface phase has been determined using scanned-energy mode photoelectron diffraction (PhD) from the Mn 2p_{3/2} core level. The results confirm the earlier finding of a quantitative LEED study, namely that the surface layer comprises an ordered, strongly corrugated two-dimensional alloy in which the Mn atoms occupy substitutional sites. By using near-grazing as well as near-normal emission directions, the PhD data are found to be sensitive to the locations of both the alloy (approximately coplanar) and the underlying substrate Cu atoms relative to the Mn emitter. This can be seen both in direct ‘projection method’ data inversion maps of the emitter environment and in full multiple-scattering simulations. The PhD data indicate a large outward relaxation of the Mn atoms relative to the surrounding alloy-layer Cu atoms (0.39 ± 0.08 Å), but this is consistent with the previous LEED study within the quoted precisions. There are, however, statistically significant differences between the LEED and PhD conclusions regarding some of the structural parameter values, most notably the layer spacing of the Mn atoms to the underlying pure Cu substrate layer.

1. Introduction

During the last few years there has been growing interest in the novel magnetic properties which can be associated with surfaces and ultra-thin films of transition and rare-earth metals, including artificial multilayer structures of ferromagnetic and non-magnetic materials which show giant magnetoresistance [1, 2]. It has recently been suggested that the Cu(100)c(2 × 2)–Mn surface structure is the first of a new class of surface alloy phases for which there is a direct connection between the magnetic and structural properties [3]. This structure has been shown to comprise an ordered, strongly corrugated single-layer alloy of CuMn stoichiometry formed by 0.5 ML of Mn on the Cu(100) surface [3, 4]. Both the stability of this surface alloy (bulk alloys of Cu and Mn show no tendency to order at the composition CuMn) and the strong corrugation (with the Mn atoms moved out from the surface) have been attributed to the magnetic properties of the Mn atoms. In particular, calculations [3] based on paramagnetic and ferromagnetic surface structures revealed that the ferromagnetic surface had a much lower energy and adopted the strongly corrugated substitutional alloy found in an associated quantitative low-energy electron diffraction (LEED) study [5]. One feature of this ferromagnetic phase is a high local magnetic moment on the Mn atoms. In this regard we should note that dilute bulk alloys of Mn in Cu are known to form spin glasses [4] in which the Mn atoms retain the high local moment of the isolated atoms;

this local moment is quenched through Mn–Mn interactions in bulk Mn metal. There is now ample experimental evidence, both indirect and direct, that Mn atoms do retain a large local moment in the Cu(100)c(2 × 2)–Mn surface alloy phase [6–9], although the system is not ferromagnetically ordered [6–8]. It appears that magnetic ordering contributes little to the energetic stability of the structure [10], and that it is the high local moment (and enhanced atomic size relative to the paramagnetic case) which is of primary importance. Nevertheless, a very similar structure, Ni(100)c(2 × 2)–Mn is found to be ferromagnetically ordered [8, 9] despite the antiferromagnetism of the associated bulk alloy.

The quantitative LEED investigation [3, 4] which first identified the Cu(100)c(2 × 2)–Mn phase concluded that the corrugated alloy surface involves Mn atoms lying 0.30 Å farther from the substrate than the Cu atoms in the same outermost atomic layer, in good agreement with the (ferro)magnetic surface calculation. STM studies of this phase have seen different degrees of corrugation in the images [11, 12]. Noh *et al* [11] actually call into question the results of the quantitative LEED study, although the relationship between the STM corrugation (electronic structure) and the geometrical corrugation (ion core positions) is, of course, far from clear. To investigate this further, we have conducted a structural study of this same surface phase using the technique of scanned-energy mode photoelectron diffraction (PhD). Our motivation for this study is twofold. Firstly, we wish to provide an independent determination of the structure by a significantly different method. Although LEED is in many ways the benchmark for the determination of long-range ordered surface structures, cases in which LEED results have conflicted with the results of other methods have not always been resolved in favour of the LEED analysis. Secondly, there are some technical issues concerned with the PhD technique, both general and specific to the present system, which we wish to resolve. The PhD technique [13, 14] utilizes the coherent interference between the component of the photoelectron wave field emitted directly from a core level of a surface atom and components of the same wave field elastically scattered from the surrounding atoms. By scanning the photon energy, and thus the photoelectron energy and wavelength, specific scattering paths contribute alternately constructively and destructively to the detected signal in a particular direction. The technique exploits mainly back-scattering, and the dominant scattering paths which contribute to the signal are those corresponding to near-180° scattering events. For the present system this technique offers one specific advantage and one potential disadvantage.

The potential advantage over LEED arises from the fact that by utilizing photoemission from a Mn core level (the 2p_{3/2}) we selectively sample the local geometry of the Mn atoms in the surface, and are thus sensitive specifically to the Mn sites and especially to the Mn distance to the underlying layer of Cu atoms. By contrast, LEED distinguishes Mn and Cu atoms only by their (relatively small) differences in elastic scattering properties. LEED should therefore be far more sensitive to the existence of a corrugation in the Cu–Mn top layer than to the sign of this corrugation (i.e. whether it is the Cu or Mn atoms which are outermost). In this regard we note that the LEED analysis of the Cu(100)c(2 × 2)–Mn surface [4] did include an evaluation of the Mn concentration in different layers which involves using these small differences in scattering properties, but the sensitivity of the results to these parameters was not presented. We can certainly expect that CuMn (for which the atomic numbers of the two constituents are very similar) must present a far more difficult problem for LEED compositional analyses than PtFe, PtNi and PtCo for which the methodology was established [15]. We also note that despite this sophisticated investigation of the Mn depth distribution (which concluded there is essentially no Mn below the outermost layer) the structural search appears not to have included the structure formed by switching the Mn and Cu atoms in the optimum structure.

By contrast, a potential difficulty for PhD in the present case is that due to the sensitivity of PhD to 180° back-scattering the technique may not be very sensitive to the location of scatterer atoms which are approximately coplanar with the emitter, because the back-scattering condition is only met for these atoms at grazing emission angles. The present case, therefore, offers an interesting test of the ability to detect (and locate) near-coplanar atoms; we find that at relatively grazing emission (70° to the surface normal) we are able to locate the Cu atoms of the top (alloy) layer. Our results confirm the main qualitative conclusions of the earlier LEED study concerning the substitutional Mn sites and the sign of the surface corrugation, but subtle quantitative differences exist, the significance of which is discussed.

2. Experimental details

The experiments were performed at the BESSY synchrotron radiation source in Berlin, taking light from the source through the Fritz Haber Institute's high-energy toroidal grating monochromator [16]. The purpose-built ultra-high-vacuum spectrometer system used was fitted with the usual facilities for *in-situ* sample preparation and characterization. The Cu(100) surface was prepared by the usual combination of x-ray Laue alignment, spark machining, mechanical polishing and *in-situ* argon ion bombardment and annealing cycles. A clean and well ordered surface was obtained as judged by synchrotron radiation core level photoemission and qualitative LEED observations. The c(2 × 2)-Mn surface structure was prepared by evaporating Mn onto the clean Cu(100) surface at room temperature to produce a sharp low-background c(2 × 2) LEED pattern.

PhD data were obtained at a sample temperature of approximately 130 K by collecting electron energy spectra which were 80 eV wide centred around the Mn 2p_{3/2} and 2p_{1/2} photoemission peaks, at photon energy steps of 2 eV in the kinetic energy range of approximately 80–480 eV in a variety of emission directions. For this purpose a VG Scientific concentric spherical sector analyser (mean radius, 152 mm) fitted with three channeltrons for parallel detection was installed in the (horizontal) plane of incidence of the synchrotron radiation at an angle of 60° to the incident radiation. Different emission directions were selected by rotating the crystal about a vertical axis to change the polar emission angle and about the crystal surface normal to change the azimuthal angle of incidence and emission. The two (2p_{1/2} and 2p_{3/2}) photoemission peak areas were obtained from the individual electron energy spectra by fitting with a spline background and two Gaussian peaks. Each resulting peak area versus photoelectron peak energy curve was normalized by a smooth spline to obtain PhD modulation spectra as described previously [17]. PhD spectra of this kind were collected at polar emission angles from 0° (normal emission) to 70° in the two principal azimuths [010] and [011], and a subset of these spectra, as described below, were used to determine the surface structure. Because of the better signal-to-noise ratio, PhD spectra from the Mn 2p_{3/2} peak were used in this analysis.

3. Results and structure determination

In order to obtain the surface structure from the PhD spectra we adopt a two-stage analysis procedure. The first stage involves a direct inversion of the experimental data to provide approximate information on the most probable locations of the nearest-neighbour back-scatterers to the (Mn) emitter atoms. In the second stage a full multiple-scattering simulation of the experimental data is used, iterating the trial structure used in the simulations to

optimize the fit. This second stage is very similar in methodology to that used in quantitative LEED studies. The first stage, on the other hand, is intended to fulfil a similar role to that of Fourier transforms of x-ray diffraction data, although the underlying theory is intrinsically more approximate in character because of the role of multiple-scattering and electron-scattering phase shifts. For both stages we use a set of PhD spectra which is representative of the dominant information provided by the method and which is of sufficient size to give a reasonable precision and degree of uniqueness in the final solution. The data set used is selected to cover as wide a range of emission geometries as possible, concentrating on directions which show particularly strong modulations or correspond to key symmetry or back-scatterer directions for possible adsorption sites. In the present case the data set used comprised polar emission angles 0° , 40° , 50° and 60° in the [010] azimuth and 20° , 60° and 70° in the [011] azimuth.

The direct methods that we use exploit the fact that, owing to the dominance of 180° back-scattering events in PhD, spectra recorded in a back-scatterer–emitter emission direction are dominated by the associated short single-scattering path length difference [18]. In the simplest procedure, Fourier transforms are taken of a large number of PhD spectra in order to identify the directions in which there is a dominant short effective path length difference indicative of near-neighbour back-scattering [19,20]. A refinement of this method, which appears to be successful with a smaller set of experimental spectra and which can also give more reliable near-neighbour distances, is the so-called projection method [21,22]. In this method the Fourier transform is replaced by a projection onto a single-scattering modulation function for an atom of the substrate species located in different possible sites on a three-dimensional grid around the emitter. The projection integral values from PhD spectra recorded in several different emission directions then are added in an exponential fashion to produce a three-dimensional ‘image’ of the most probable locations of back-scatterer atoms. A full and more exact description of the method has been given elsewhere, together with examples of its successful application to a range of experimental systems (see, e.g. [22,23]).

In the present case of the Cu(100) $c(2 \times 2)$ –Mn system, the results of applying the projection method in order to identify the nearest-neighbour back-scatterers to the surface Mn atoms are shown in figure 1 in the form of two-dimensional grey-scale sections of the half-space below these emitters. Figure 2 shows a schematic model of the structure deduced from these results (and confirmed by the full simulations) for comparison. In figure 1 two cuts are shown perpendicular to the surface passing through the Mn emitter atom located at (0, 0, 0): one in the [011] azimuth and the other in the [010] azimuth. In the former, two symmetrically equivalent features can be seen approximately 0.5 \AA below the emitter. A cut parallel to the surface at this depth shows that there are four features which appear in the appropriate azimuthal directions and at the correct lateral displacements to be associated with coplanar atoms in a layer having the periodicity of Cu(100)—exactly the behaviour to be expected if the Mn emitter atoms occupy substitutional sites ‘in’ (but strictly a few tenths of an ångström above) the outermost Cu layer. The vertical cut in the [010] azimuth, by comparison, shows two symmetrically equivalent features about 2 \AA below the emitter. A cut parallel to the surface at this depth shows the location of the four nearest-neighbour Cu atoms in the layer expected for this same substitutional site. The projection method results thus provide strong evidence that the substitutional surface alloy geometry found by LEED is correct with the Mn atoms lying at a larger layer spacing than the outermost Cu atoms. The results also show that the PhD method is capable of detecting the presence of the near-coplanar Cu atoms of the top alloy layer.

To check the validity of this preliminary site assignment, and to provide a more

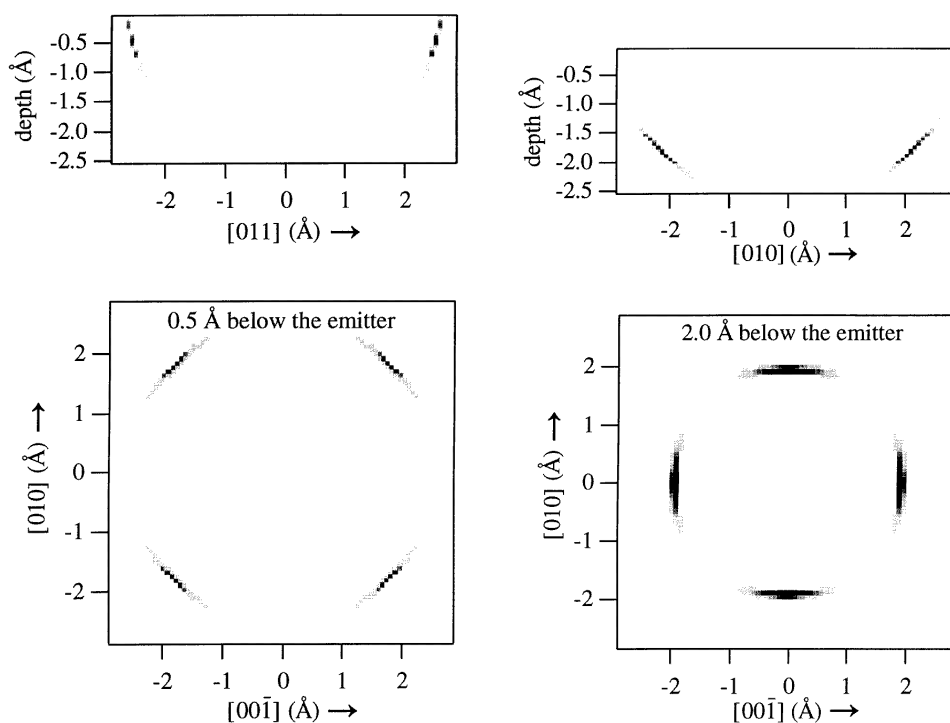


Figure 1. Results of the application of the 'projection method' of direct inversion of the PhD spectra to obtain a three-dimensional map of the most probable location of the nearest-neighbour substrate back-scatterer atoms to the Mn emitters. The upper diagrams show cuts perpendicular to the surface passing through the emitter, located at $(0, 0, 0)$, in the two principal azimuths $[100]$ and $[010]$. The lower diagrams show cuts parallel to the surface at different depths below the emitter chosen to intersect the main features seen in the perpendicular cuts.

quantitative determination of the atomic locations in the near-surface region, a second stage of analysis used full multiple-scattering simulations of the data and iteration of the structural parameters. Full details of this methodology have been given elsewhere, but the key features are as follows.

(i) The multiple-scattering calculations are based on a magnetic quantum number expansion and incorporate the effects of both the finite energy and the angular resolution of the measurements which also speeds the convergence [24–27].

(ii) An objective reliability factor (R-factor), a normalized sum of the squares of the deviations of theoretical and experimental modulation amplitudes, is used as a criterion of the best fit. This R-factor [28] is normalized such that perfect agreement corresponds to a value of 0, uncorrelated data to a value of 1, and anticorrelated data to a value of 2.

(iii) An approximate 'linear' computational method [27] in the multiple-scattering calculations is utilized for the purpose of searching large areas of multi-parameter space, and an automated Newton–Gauss iteration (coupled with more exact calculations) is then used to optimize the fits and the exact best-fit structural parameters.

(iv) An estimated variance, based on the size of the data set and the best-fit R-factor value, is used to determine the limits of precision. The procedure is similar to that proposed by Pendry [29] in the evaluation of LEED structural optimization.

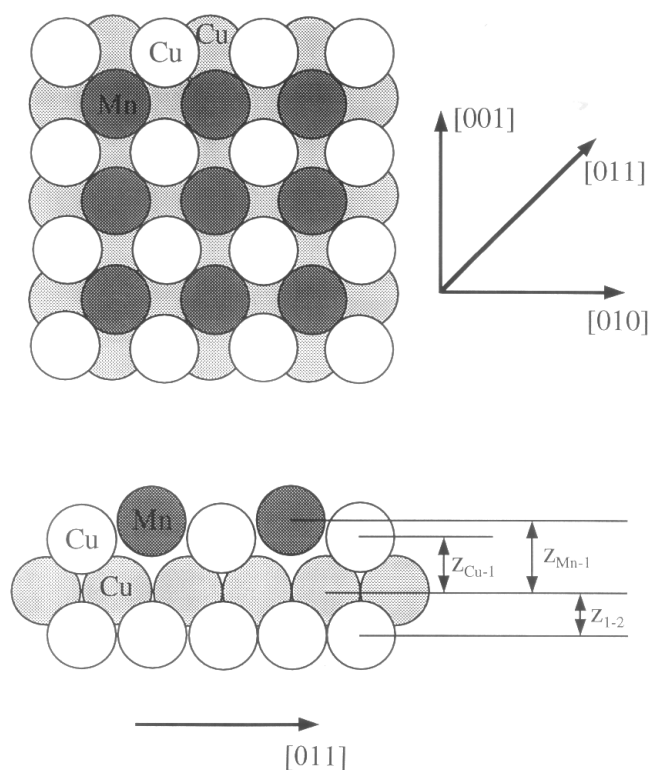


Figure 2. Schematic diagram showing plan and side views of the Cu(100) $c(2 \times 2)$ -Mn surface alloy structure found to give the best fit in the present study and in the earlier LEED analysis. The structural parameter values investigated in the present study are defined in the figure.

The results of this structural optimization are summarized in figure 3 and table 1. In particular, figure 3 shows a comparison of the best-fit theory and experimental PhD spectra, while table 1 summarizes the best-fit structural parameter values; a subset of these is defined in the schematic diagram of the structure in figure 2, while the remainder (sums or differences of these) are defined in the heading to table 1. In addition to these primary structural parameters, some optimization of the vibrational amplitudes was undertaken, leading to values for the mean-square vibrational amplitudes of the Mn atoms of 0.0029 \AA^2 parallel to the surface and 0.0060 \AA^2 perpendicular to the surface, with the (isotropic) value for the Cu atoms in the alloy layer being 0.0022 \AA^2 . The bulk Cu atom value of this vibrational amplitude was optimized at 0.0037 \AA^2 . The overall R-factor for the seven spectra (some 3000 eV of energy-scan spectra) is 0.23; the best individual spectral R-factor value is 0.11 and the worst 0.34. These values represent a very good fit from our experience. Structural models other than this substitutional surface alloy yielded much worse fits. For example, simple Mn overlayers based on atop or bridge sites gave global R-factors greater than 0.8. Simple $c(2 \times 2)$ overlayers based on hollow site occupation by Mn atoms alone, or by a mixture of Cu and Mn atoms, also led to significantly worse fits. In particular, while comparable fits with those for the substitutional alloy were obtained for the near-normal emission spectra, the fit to the 70° [011] spectrum was much worse (R-factor of 0.82 compared with 0.23 for the surface alloy); this result shows clearly how this grazing

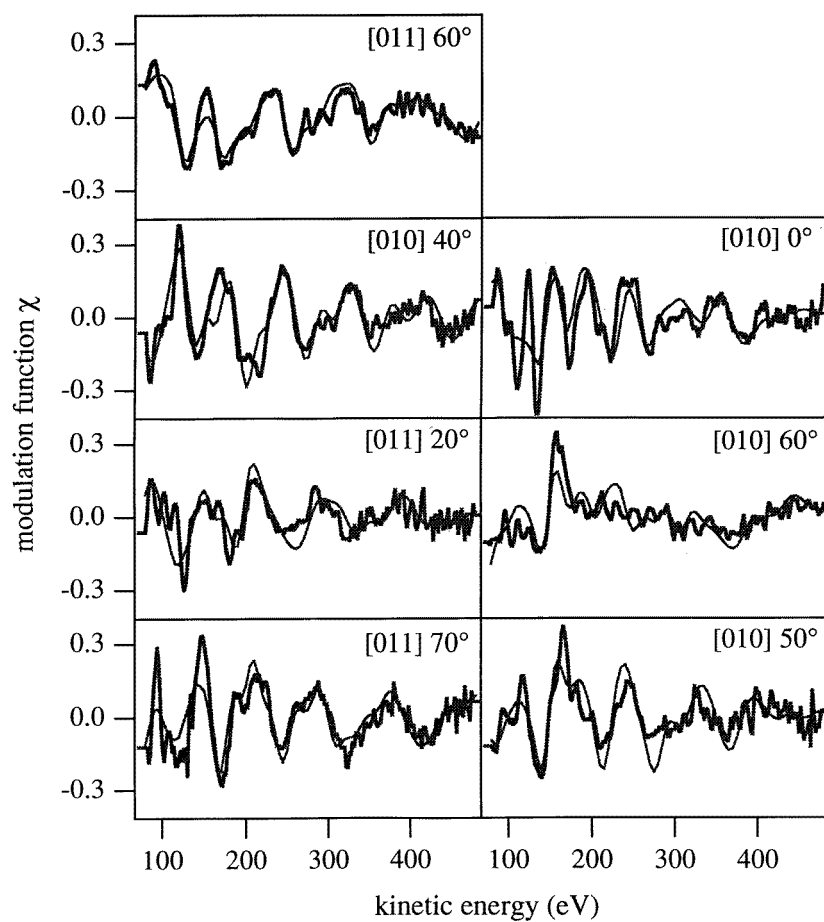


Figure 3. Comparison of the seven experimental PhD spectra used in the full structural analysis with theoretical simulations obtained for the best-fit structure as defined in table 1.

emission spectrum picks out the back-scattering from the Cu atoms of the alloy layer which are missing in the simple overlayer.

Also shown in table 1 are the structural parameter values given by the earlier LEED study. For the results of the present study we have distinguished in this table those parameter values to which our method is directly sensitive (the location of scatterer atoms relative to the Mn emitter atoms) and those parameter values deduced from combinations of the primary values. In the case of LEED this distinction is less clear; LEED is not based on any specific internal reference point within the structure and is sensitive to all relative layer spacings. A comparison of the LEED and PhD values in this table shows that, while the overall trends are the same in both sets, there are quantitative differences.

If we first consider the corrugation amplitude, $\Delta z_{\text{Mn-Cu}}$, of the alloy layer, an effect not easily explained by simple hard-sphere atom models and thus of primary significance relative to the spin state of the Mn atoms, we see that the two techniques agree within the estimated precisions; strictly the difference is $0.09 \pm 0.08 \text{ \AA}$ but the discrepancy is only slightly larger than one standard deviation and so cannot be regarded as particularly

Table 1. Summary of structural parameter values for the Cu(100)c(2×2)–Mn structure obtained from this work and from the previous LEED study. Several of these parameters are defined in figure 2; the remainder are sums or differences of these values: $\Delta z_{Mn-Cu} = z_{Mn-1} - z_{Cu-1}$; $z_{Mn-2} = z_{1-2} + z_{Mn-1}$. In the case of the present study the values in italics are parameter values deduced from the primary values of layer spacings relative to the Mn emitter atoms. The italicized LEED values are inferred from sums of two values given in the original paper; so the quoted error is estimated from those of the component values.

Parameter (units)	Value	
	This work	LEED
z_{Mn-1} (Å)	2.02 ± 0.04	2.09 ± 0.02
z_{Cu-1} (Å)	1.63 ± 0.08	1.79 ± 0.02
Δz_{Mn-Cu} (Å)	0.39 ± 0.08	0.39 ± 0.02
z_{1-2} (Å)	1.83 ± 0.08	1.80 ± 0.03
z_{Mn-2} (Å)	3.85 ± 0.08	3.99 ± 0.04
Δz_1 (Å)	—	0.02 ± 0.03

significant. Although PhD is sensitive to the sign of this corrugation, it is less sensitive than LEED to the actual value. This is because LEED is sensitive to the layer spacing directly, whereas PhD can only locate the near-coplanar Cu atoms through a near-grazing emission geometry and is thus sensitive to the Mn–Cu nearest-neighbour distance; for the near-coplanar geometry a small error in this distance leads to a much larger imprecision in the layer spacing. More significant differences between the PhD and LEED results are seen, however, in the layer spacings of the top-layer Mn atoms relative to the lower Cu layers of the substrate. The spacings from the Mn atoms to the first complete layer of Cu atoms differ by 0.07 \AA , whereas the combined estimated errors for this difference are only $\pm 0.04 \text{ \AA}$. Near-normal emission PhD spectra are particularly sensitive to this value, but of course LEED too is especially sensitive to outermost layer spacings. This relatively small difference is thus significant but unexplained. A similar discrepancy exists in the spacing from the Mn atoms to the Cu atoms in the second layer of the substrate ($0.14 \pm 0.09 \text{ \AA}$). One consequence of these values is that the PhD data imply a rather large contraction of the spacing of the outermost Cu atoms (in the alloy layer) to the first complete Cu atomic layer; at 1.63 \AA this value represents a 10% reduction relative to the bulk Cu–Cu layer spacing. Of course the precision is relatively low ($\pm 0.08 \text{ \AA}$ or $\pm 4\%$) because in the PhD experiment this value is obtained from the difference in the Mn–Cu atom layer spacings, and the near-coplanar location of the alloy Cu atoms means that this layer is not very precisely located, as explained above. Nevertheless, the PhD results do indicate that the outermost Mn atoms are significantly closer to the underlying Cu substrate (both first and second layers of this substrate) than is indicated by the LEED results. The reason for this discrepancy is unclear and may warrant further study. In view of the indirect means of locating the outermost Cu–Cu layer spacing, however, by far the most significant discrepancy relative to the LEED result is the spacing from the Mn to the underlying Cu substrate layer, and it would be interesting to provide a further independent test of this parameter.

4. Conclusions

Our scanned-energy mode PhD investigation of the structure of the Cu(100)c(2×2)–Mn surface phase provides independent confirmation of the main features of the previous LEED

study of this system. Specifically, the surface comprises a substitutional surface alloy in which the Mn atoms lie significantly farther from the surface than the outermost Cu atoms. There is also reasonable quantitative agreement with LEED over the amplitude of this surface corrugation. Both the alloy phase stability and the corrugation amplitude have been attributed to the high-spin state of the Mn atoms which have a large resultant magnetic moment. Our investigation has also demonstrated the viability of the PhD method as a means of investigating near-coplanar surface layers, despite its reliance on near-180° back-scattering for structural information. There are, however, some small but significant differences in the quantitative conclusions of this study and the previous LEED investigation, most notably in the layer spacing of the Mn atoms in the surface alloy layer relative to the underlying pure Cu layer. Only an investigation by a further independent technique is capable of resolving this discrepancy.

Acknowledgments

The authors are pleased to acknowledge the financial support of this work in the form of grants from the Engineering and Physical Science Research Council (UK), the European Community through the Human Capital and Mobility Networks (grant ERBCHRX CT930358) and Large-Scale Facilities programmes and the Bundesministerium für Bildung und Forschung under contract 05 625EBA 6.

References

- [1] See, e.g., Allenspach R 1994 *J. Magn. Magn. Mater.* **129** 160
- [2] See, e.g., Seigmann H C 1992 *J. Phys.: Condens. Matter* **4** 8395
- [3] Wuttig M, Gauthier Y and Blügel S 1993 *Phys. Rev. Lett.* **70** 3619
- [4] Wuttig M, Knight C C, Flores T and Gauthier Y 1993 *Surf. Sci.* **292** 189
- [5] See, e.g., Mydosh J A 1994 *J. Appl. Phys.* **129** 160
- [6] O'Brien W L, Zhang J and Tonner B P 1993 *J. Phys.: Condens. Matter* **5** L515
- [7] O'Brien W L and Tonner B P 1994 *J. Appl. Phys.* **76** 6468
- [8] O'Brien W L and Tonner B P 1995 *Phys. Rev. B* **51** 617
- [9] Hayden A B, Pervan P and Woodruff D P 1995 *J. Phys.: Condens. Matter* **7** 1139
- [10] Wuttig M, Feldmann B and Flores T 1995 *Surf. Sci.* **331-3** 659
- [11] Noh H P, Hashizume T, Jeon D, Kuk Y, Pickering H W and Sakurai T 1994 *Phys. Rev. B* **50** 2735
- [12] van der Kraan R G P and van Kempen H 1995 *Surf. Sci.* **338** 19
- [13] Woodruff D P and Bradshaw A M 1994 *Rep. Prog. Phys.* **57** 1029
- [14] Bradshaw A M and Woodruff D P 1995 *Applications of Synchrotron Radiation: High-resolution Studies of Molecules and Molecular Adsorbates on Surfaces* ed W Eberhardt (Berlin: Springer) p 127
- [15] Gauthier Y, Baudoing R, Lundberg M and Rundgren J 1987 *Phys. Rev. B* **35** 7867
- [16] Dietz E, Braun W, Bradshaw A M and Johnson R 1985 *Nucl. Instrum. Methods A* **239** 359
- [17] Schindler K-M, Fritzsche V, Asensio M C, Gardner P, Ricken D E, Robinson A W, Bradshaw A M, Woodruff D P, Conesa J C and González-Elipe A R 1992 *Phys. Rev. B* **46** 4836
Hofmann Ph, Schindler K-M, Bao S, Fritzsche V, Ricken D E, Bradshaw A M and Woodruff D P 1994 *Surf. Sci.* **304** 74
- [18] Dippel R, Woodruff D P, Hu X-M, Asensio M C, Robinson A W, Schindler K-M, Weiss K-U, Gardner P and Bradshaw A M 1992 *Phys. Rev. Lett.* **68** 1543-6
- [19] Fritzsche V and Woodruff D P 1992 *Phys. Rev. B* **46** 16128
- [20] Schindler K-M, Hoffman Ph, Fritzsche V, Bao S, Kulkarni S, Bradshaw A M and Woodruff D P, 1993 *Phys. Rev. Lett.* **71** 2054
- [21] Hofmann Ph and Schindler K-M 1993 *Phys. Rev. B* **47** 13941
- [22] Hofmann Ph, Schindler K-M, Bao S, Bradshaw A M and Woodruff D P 1994 *Nature* **368** 131
- [23] Hofmann Ph, Schindler K-M, Fritzsche V, Bao S, Bradshaw A M and Woodruff D P 1994 *J. Vac. Sci. Technol. A* **12** 2045-50
- [24] Fritzsche V 1990 *J. Phys.: Condens. Matter* **2** 9735

- [25] Fritzsche V 1992 *J. Electron Spectrosc. Relat. Phenom.* **58** 299
- [26] Fritzsche V 1992 *Surf. Sci.* **265** 187
- [27] Fritzsche V and Pendry J B 1993 *Phys. Rev. B* **48** 9054
- [28] Dippel R, Weiss K-U, Schindler K-M, Gardner P, Fritzsche V, Bradshaw A M, Asensio M C, Hu X M, Woodruff D P and González-Elipe A R 1992 *Chem. Phys. Lett.* **199** 625
- [29] Pendry J B 1980 *J. Phys. C: Solid State Phys.* **13** 937